College of Engineering

Stabilization of Liquefiable Soils Using Colloidal Silica Grout

Patricia M. Gallagher, A.M.ASCE[1]; Ahmet Pamuk[2]; and Tarek Abdoun, A.M.ASCE[3]

Abstract: Passive site stabilization is a new technology proposed for nondisruptive mitigation of liquefaction risk at developed sites susceptible to liquefaction. It is based on the concept of slowly injecting colloidal silica at the edge of a site with subsequent delivery to the target location using natural or augmented groundwater flow. Colloidal silica is an aqueous dispersion of silica nanoparticles that can be made to gel by adjusting the pH or salt concentration of the dispersion. It stabilizes liquefiable soils by cementing individual grains together in addition to reducing the hydraulic conductivity of the formation. Centrifuge modeling was used to investigate the effect of colloidal silica treatment on the liquefaction and deformation resistance of loose, liquefiable sands during centrifuge in-flight shaking. Loose sand was successfully saturated with colloidal silica grout and subsequently subjected to two shaking events to evaluate the response of the treated sand layer. The treated soil did not liquefy during either shaking event. In addition, a box model was used to investigate the ability to uniformly deliver colloidal silica to loose sands using low-head injection wells. Five injection and two extraction wells were used to deliver stabilizer in a fairly uniform pattern to the loose sand formation. The results of the box model testing will be used to design future centrifuge model tests modeling other delivery methods of the grout.

DOI: 10.1061/(ASCE)0899-1561(2007)19:1(33)

CE Database subject headings: Liquefaction; Soil stabilization; Grouting; Colloids.

Introduction

Liquefaction is a phenomenon marked by a rapid and dramatic loss of soil strength, which can occur in loose, saturated soil deposits subjected to earthquake motions. Certain types of soil deposits, such as sand deposits, hydraulic fills, and mine tailings dams are particularly susceptible to liquefaction. The onset of liquefaction is usually sudden and dramatic and can result in large deformations and settlements, floating of buried structures, or loss of foundation support. Lateral spreading is a related phenomenon characterized by lateral movement of intact soil blocks over shallow liquefied deposits. Displacements caused by lateral spreading can range from minor to quite large. Gently sloping areas along waterfronts are most susceptible to lateral spreading. As a consequence, bridges and other waterfront infrastructure can be damaged significantly due to lateral spreading.

Structural damage due to liquefaction-induced ground failure is a very costly phenomenon. More than 250 bridges were damaged by this phenomenon during the 1964 Alaskan earthquake. Much of the billion dollars in damage caused by the 1964 Niigata earthquake in Japan can be attributed to widespread liquefaction-induced lateral spreading. More recent events, including damage to shallow and deep foundations and port facilities include the 1983 Nihonkai-Chubu earthquake in Japan, the 1989 Loma Prieta and 1996 Northridge earthquakes in California, the 1990 Philippines and 1991 Costa Rica earthquakes, and the 1995 Kobe earthquake in Japan. Liquefaction and lateral spreading caused billions of dollars in damage to port facilities in the January 1995 Kobe event (NRC 1985; Hamada et al. 1986, 1996; Hamada and O'Rourke 1992; O'Rourke and Hamada 1992; Bartlett and Youd 1992; Arulanandan and Scott 1993; Ishihara et al. 1996; Dobry and Abdoun 1998, 2001).

At sites susceptible to liquefaction, the simplest way to mitigate the liquefaction risk is to densify the soil. For large, open, and undeveloped sites, the easiest and least expensive method of ground improvement is densification by "traditional" methods of ground improvement such as deep dynamic compaction, explosive compaction, or vibrocompaction. At constrained or developed sites, ground improvement by densification may not be possible due to the presence of structures sensitive to deformation or vibration. Additionally, access to the site may be limited and normal site use could interfere with mitigation activities. At these sites, the most common methods of ground improvement are underpinning or grouting. These methods target specific structures rather than the entire site. With underpinning, structural elements are used to provide additional support for the structure. In the case of grouting, the typical method is to inject grout under pressure through closely spaced boreholes. Typical grout materials include cement or various chemicals such as sodium silicate that are formulated with short set (gel) times. These materials tend to have a high viscosity, so they are often used to form grout columns rather than to permeate the entire area beneath the structure.

Passive site stabilization is a new technology proposed for remediation of liquefaction risk at developed sites susceptible to liquefaction (Gallagher et al. 2002; Gallagher and Koch 2003). It

[1]Assistant Professor, Dept. of Civil, Architectural, and Environmental Engineering, Drexel Univ., 3141 Chestnut St., Philadelphia, PA 19104 (corresponding author). E-mail: pmg24@drexel.edu

[2]Postdoctoral Research Fellow, Dept. of Civil Engineering and Engineering Mechanics, Columbia Univ., 610 Mudd, 500 West 120th St., New York, NY 10027.

[3]Assistant Professor and Manager, RPI Geotechnical Centrifuge Research Center, Dept. of Civil Engineering, Rensselaer Polytechnic Institute, JEC 4049, Troy, NY 12180-3590.

Note. Associate Editor: Hilary I. Inyang. Discussion open until June 1, 2007. Separate discussions must be submitted for individual papers. To extend the closing date by one month, a written request must be filed with the ASCE Managing Editor. The manuscript for this paper was submitted for review and possible publication on February 11, 2005; approved on July 29, 2005. This paper is part of the ***Journal of Materials in Civil Engineering***, Vol. 19, No. 1, January 1, 2007. ©ASCE, ISSN 0899-1561/2007/1-33–40/$25.00.

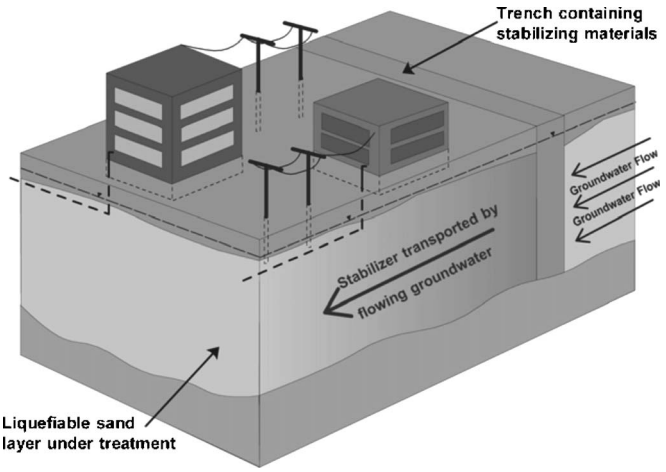

Fig. 1. Passive site stabilization for mitigation of liquefaction risk

is based on slowly injecting colloidal silica at the upgradient edge of a site, with subsequent delivery of the stabilizer to the target location via groundwater flow (Fig. 1). Low-head extraction wells can be used to adjust the groundwater flow pattern for targeted delivery of the stabilizer to the entire site. Colloidal silica acts to stabilize the soil by both cementing individual grains together and by reducing the overall hydraulic conductivity of the formation. In this method, an entire site can be treated, including both structures and lifelines. Relying on low-gradient stabilizer delivery instead of the traditional high-pressure injection of grout requires that the stabilizer have a low initial viscosity, a long induction period (during which the viscosity stays fairly low), and long gel times (on the order of 50–100 days). In a 5% by weight dilution, the material cost of colloidal silica is expected to be similar to the cost of microfine cement. Installation costs are expected to be significantly lower than the costs associated with typical cement grouting.

Colloidal silica has been investigated for use in stabilizing sands by Yonekura and Kaga (1992), Persoff et al. (1999), Gallagher and Mitchell (2002), and Liao et al. (2003). Yonekura and Kaga (1992) proposed colloidal silica as a replacement for the most commonly used chemical grout, sodium silicate. Persoff et al. (1999) investigated the effect of dilution on the strength and hydraulic conductivity of sand treated with colloidal silica. Gallagher and Mitchell (2002) studied the liquefaction resistance of loose sands treated with colloidal silica in percentages that varied from 5 to 20% by weight. Liao et al. (2003) also studied the liquefaction resistance of sand stabilized with colloidal silica. Gallagher et al. (2002) used centrifuge modeling to examine the ability of colloidal silica treatment to increase the liquefaction resistance and reduce the deformation of loose sands. Gallagher and Koch (2003) reported results of box model experiments in which low-head injection wells were used to deliver colloidal silica to loose sands.

This paper describes the use of centrifuge modeling to investigate the effects of colloidal silica treatment on the liquefaction and deformation properties of loose, liquefiable sands during centrifuge in-flight shaking. Loose Nevada No. 120 sand was saturated with 6% by weight colloidal silica stabilizer and subsequently subjected to two shaking events that simulated earthquake motions with uniform peak accelerations of 0.2 and 0.25g. The treated sand layer did not liquefy during either shaking event. In addition, significantly lower levels of strains (1/2–1%) were measured for the treated centrifuge models compared to the strains (3–6%) recorded in similar centrifuge tests done on untreated soil models (Taboada 1995).

This paper also describes the use of box modeling to investigate the delivery of dilute colloidal silica stabilizer through loose sand deposits under small gradients imposed by injection and extraction wells. Five injection and two extraction wells were used to deliver about $1\frac{1}{2}$ pore volumes of 5% by weight colloidal silica to the sand over a period of about 10 h. During delivery, the concentration profile across the model was monitored. The purpose of this work was to identify the key parameters affecting colloidal silica delivery during the box model experiment. The results of this and other box model experiments will be used to design additional centrifuge tests that will model the injection process during flight.

Colloidal Silica

Colloidal silica is an aqueous dispersion of silica nanoparticles (7–22 nm) produced from saturated solutions of silicic acid. When diluted to 5% by weight, colloidal silica solutions have a density and viscosity similar to water (about 15–20 $Pa^4.s$; water=10 $Pa^4.s$). Colloidal silica solutions can have long induction periods during which the viscosity remains fairly low, as well as long, controllable gel times of up to a few months. Colloidal silica is also nontoxic, biologically, and chemically inert, and has excellent durability characteristics, making it an outstanding candidate for a stabilizer. The colloidal silica used for this research was Ludox-SM, which was purchased from Grace Davison of Columbia, Maryland. It is supplied as a 30% by weight silica solution with a viscosity of 55 $Pa^4.s$, a pH of 10, and an average particle size of 7 nm.

Colloidal silica nanoparticles form when H_4SiO_4 molecules interact to form siloxane (Si–O–Si) bonds with other molecules. The surfaces of the particles contain uncombined silanol (SiOH) groups (Iler 1979). When the particles interact with other particles, they form interparticle siloxane bonds, as shown in Fig. 2(b). When the particles grow to the desired size, the solution can be stabilized by increasing the pH to prevent further particle growth. The increase in pH causes the particles to ionize and repel each other. Gelation can be induced at a later time by reducing the repulsive forces in a controlled manner, which allows the colloidal particles to coagulate, increase in size, and eventually form a firm gel. The gel time is determined by the rate of particle-to-particle interaction.

Alkaline solutions such as sodium hydroxide are often used to stabilize colloidal silica solutions and prevent them from gelling. The alkali reacts with the surfaces of the particles, creating a negative charge on the particles and causing them to repel each other. This process is shown in Fig. 2(a). The hydroxyl ions added by the alkaline solution would actually catalyze gel formation, but at high pH the colloidal silica is stable because of its high particle charge. At lower pH values, the particle charge decreases in proportion to the concentration of hydroxyl ions in solution. Therefore, the particles can interact and form siloxane bonds as depicted in Fig. 2(b). The result is that the minimum gel time occurs between pH 5 and 6. As the pH continues to drop below 5, the hydroxyl ions disappear and the particles become uncharged, as shown in Fig. 2(c). Therefore, the rate of siloxane bond formation decreases and there is a corresponding increase in gel time.

The factors controlling the gel time of colloidal silica include the silica solids content, the pH, and the ionic strength of the diluted colloidal silica solution. For a given silica content, the gel

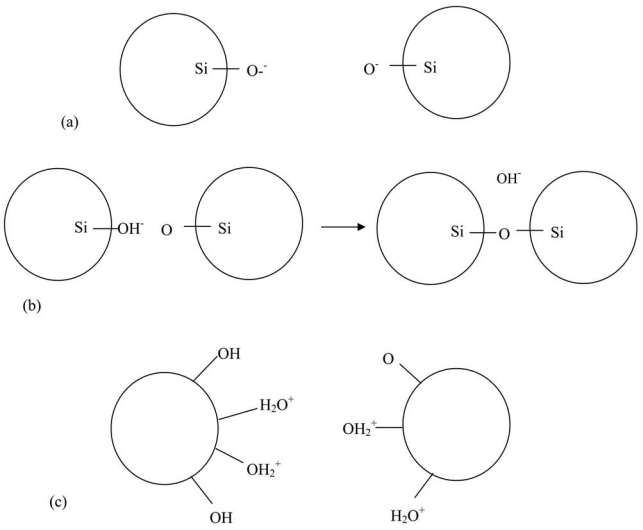

Fig. 2. Behavior of colloidal silica particles at different pH values: (a) pH≥8: O^- on surface causes particles to repel each other; (b) 5 <pH<8: O^- on surface of one particle forms bond with H on other particle, Si–O–Si bond forms between molecules; and (c) pH<5: particles are neutral or repel each other

time can be altered by lowering the pH and changing the ionic strength of the dilute colloidal silica solution. Example gel time curves are shown in Fig. 3 for 5% by weight solutions at different ionic strengths and pH values.

In general, colloidal silica will permeate loose sand under low-head injection and extraction wells when the viscosity remains less than about 100 Pa^4.s. As the viscosity continues to increase, a firm, resonating gel forms. The gel time is defined as the time from the end of mixing until the colloidal silica forms this type of gel. The curing time is the time between the formation of a firm, resonating gel and strength testing.

Gelled colloidal silica is expected to be stable in the subsurface indefinitely. Whang (1995) estimated the lifetime of colloidal silica to be greater than 25 years, while estimating the lifetimes of sodium silicate and acrylate grouts to be between 10 and 20 years. Persoff et al. (1999) immersed samples of sand treated with colloidal silica in test liquids containing different non-aqueous phase liquids (NAPLs), water saturated with different

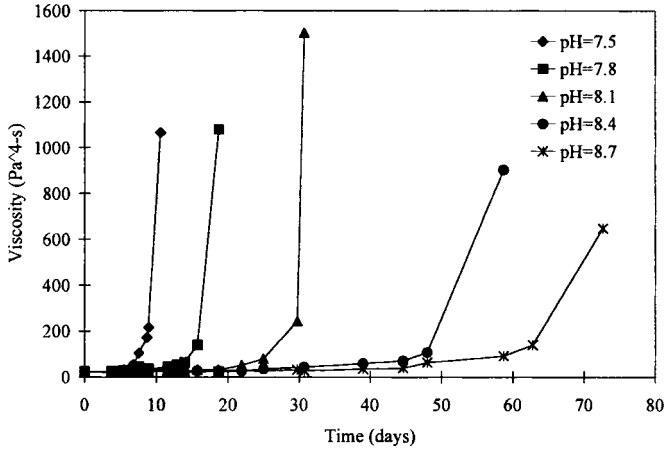

Fig. 3. Typical colloidal silica gel time curves for 5% by weight colloidal silica at 0.1 N NaCl

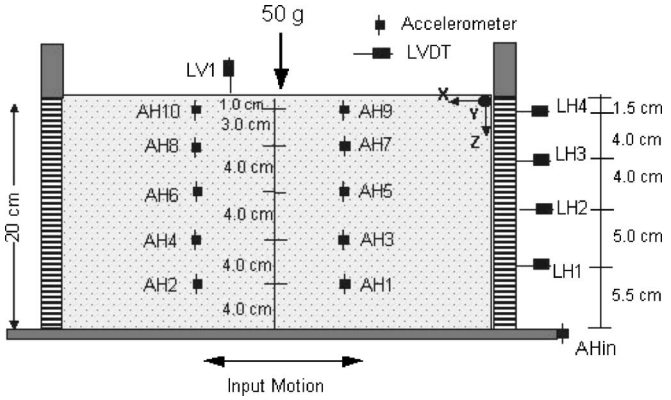

Fig. 4. Setup and instrumentation for centrifuge model

NAPL's, HCl diluted to pH 3, and aniline for 95 days. Only the sample immersed in aniline was weaker after immersion. Based on silica solubility curves (Iler 1979), colloidal silica gel is expected to have very low solubility in the subsurface as long as the pH of the groundwater remains between about 5 and 8 [Fig. 2(b)].

Centrifuge Model Preparation and Testing

A centrifuge experiment was performed at Rensselaer Polytechnic Institute (RPI) in which loose Nevada 120 sand was treated with colloidal silica grout at a concentration of 6% by weight. A sketch of RPI's laminar box, including the instrumentation used for the model, is presented in Fig. 4. The laminar box is a flexible-wall container comprising a stack of rectangular aluminum rings, separated by linear roller bearings arranged to permit relative movements between rings with minimal friction. The dimensions of the box are 460 mm by 370 mm in plan and 260 mm high. The model was prepared at a relative density of 40% by pluviating dry sand into the laminar box. The model was prepared with a medium–coarse sand drain around the grout supply ports to allow the grout to spread out evenly into the sand (Fig. 5).

For cost-effective mitigation, it is expected that only one pore volume of 5% by weight colloidal silica will be injected. However, in the interest of obtaining complete replacement of the pore water with colloidal silica, 1 1/2 pore volumes were used in both the centrifuge and the box modeling experiments. Fig. 5 shows the setup for the grouting procedure during model preparation. This grouting procedure evolved as a result of inadequate satura-

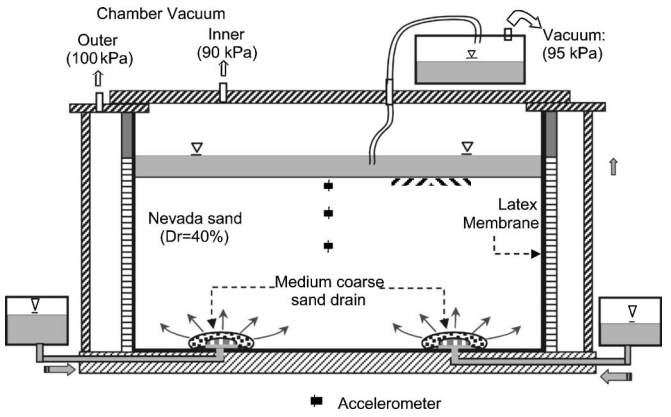

Fig. 5. Model setup for grouting

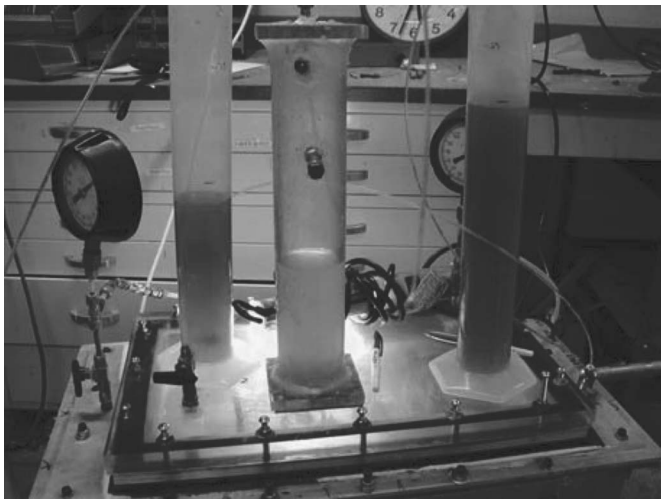

Fig. 6. Photograph of grouting setup

tion in previous experiments described by Gallagher et al. (2002). For the model used in this test, the grout was introduced through the bottom of the box and drawn up through the soil under a vacuum. The dyed grout was delivered to the model through the bottom ports during a saturation period of 13 h. Fig. 6 presents a picture of the grouting setup. The first grout emerging from the model into the overflow chamber was very light in color compared to the grout supply due to dilution with the pore water. Over time, the grout in the exit chamber became darker and eventually became the same color as the grout in the supply chamber, indicating that the grout had likely displaced the pore water and that the pores were filled with grout. Visual inspection during post-test excavation of the model revealed that the model was uniformly grouted (Fig. 7).

The gel time was selected to permit ample time for the grout to travel through the model during the saturation period. During the grouting, the viscosity increased from 15 to 17 Pa^4.s. The colloidal silica formed a firm, resonating gel about 56 h after mixing (about 43 h after the end of delivery). Prior to testing, the gel was cured for about 240 h (about four times the gel time). While the grouting method is not representative of potential field delivery techniques, the intention was to get complete grout coverage in the model. By grouting the entire soil mass, the maximum improvement that can be attained using a certain grout concentration (in this case 6% by weight) can be determined. It was intended to use 5% by weight colloidal silica; however, due to a mathematical error, the actual concentration was 6% by weight.

Fig. 7. Photograph of model excavation and uniformly grouted soil

The prototype being simulated is a loose, liquefiable sand formation that has been treated with colloidal silica. In model units, the thickness of the soil is approximately 200 mm (Fig. 4), which simulates a 10 m prototype soil deposit at 50g. At 50g, the D_r =40% fine Nevada sand layer in the model simulates a liquefiable, D_r=40% coarse Nevada sand in the prototype. The horizontal accelerations outside the laminar box and in the soil, lateral displacements of the rings, and vertical displacement of the soil were measured. The model was instrumented with five pairs of accelerometers placed at different elevations near the center of the model (Fig. 4). Five LVDTs were used to measure the lateral displacement of the rings and the vertical displacement at the top of the treated mass. Because treatment with colloidal silica grout significantly reduces the hydraulic conductivity of the treated soil, pore pressure measurements were not made. The model was excited by 20 cycles of a 2 Hz sinusoidal input parallel to the base of the laminar box, with uniform peak accelerations of 0.2 and 0.25g, in prototype units.

Centrifuge Modeling Results

Recorded Accelerations

The model was subjected to two shaking events to evaluate the response of the treated sand layer. The acceleration time histories measured at different elevations are shown in Figs. 8 and 9 for the first and second episodes of shaking, respectively. Signal amplification was observed along the depth of soil deposit during shaking events. The amplification appeared to be increasing with peak input acceleration amplitude. However, the recorded accelerations indicated that the treated soil did not liquefy during either the first or the second shaking event.

Recorded Displacements

Fig. 10 shows lateral displacement profiles for the first and second episodes of shaking. The recorded lateral displacements were measured by horizontal LVDTs mounted on the container rings at various elevations. Shear strains of ±0.5 and ±1% were recorded during the first and second shaking events, respectively. Fig. 11 shows the measured settlement during the first and second shaking event. At prototype scale, the treated soil experienced about 30 mm of settlement (0.3% strain) at the center of the model during the first episode of shaking and less than 10 mm (0.1% strain) of settlement during the second shaking episode.

Box Model Preparation and Testing

The box model used for the stabilizer delivery experiment has three compartments—a central chamber for sand placement and two outer reservoirs for groundwater control. A photograph of the box model is shown in Fig. 12. The model was constructed of 10-mm-thick plexiglas with internal dimensions of 760 mm $\times$305 mm in plan, and a height of 265 mm. The flow length through the sand was 460 mm, and each water reservoir was 150 mm in length. Screens with a No. 200 mesh size are used

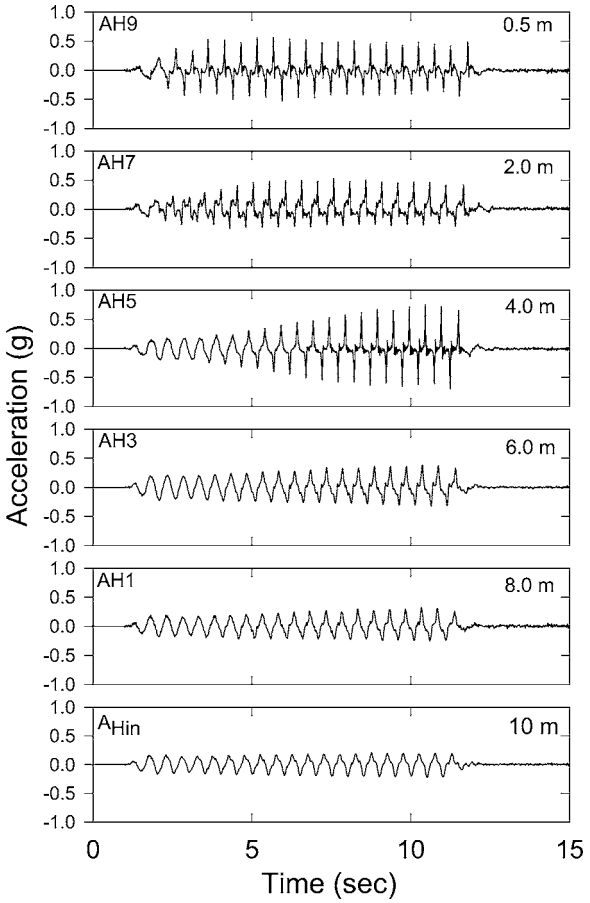

Fig. 8. Input and recorded accelerations at different depths, first shake

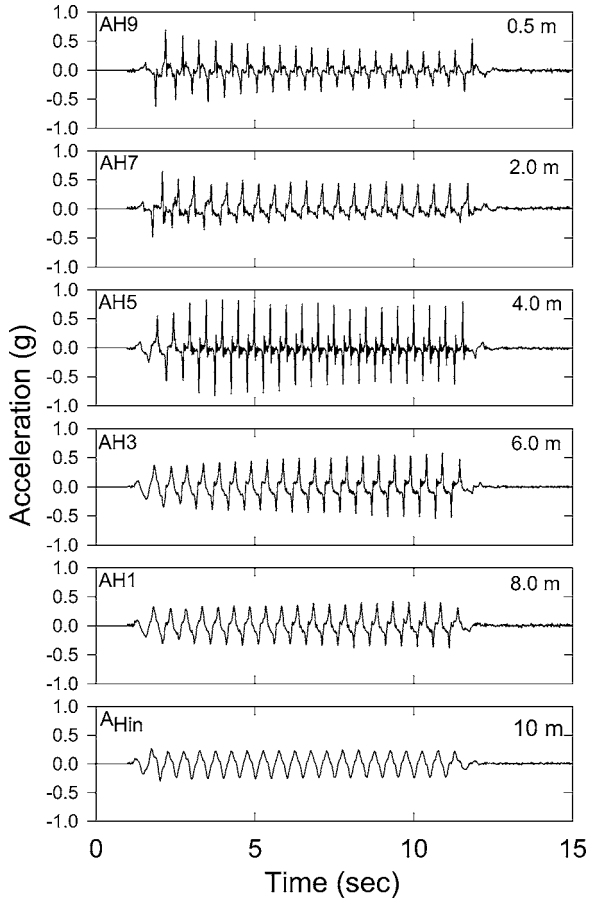

Fig. 9. Input and recorded accelerations at different depths, second shake

between the water and soil compartments to prevent soil loss from the central chamber into the reservoirs. In Fig. 12, the left and right sides of the tank were the upstream and downstream chambers, respectively. Sampling ports in the sand compartment, visible in Fig. 12, are used to extract fluid samples across the soil profile, to facilitate measuring the changes in the pore fluid chemistry as the colloidal silica was delivered to the formation. The side of the sand compartment was removed after the experiment, so that the treated sand could be excavated for visual inspection and strength testing.

The model was filled by pluviating Nevada No. 120 sand to a height of 200 mm at a relative density of 40%. After sand placement, the upstream reservoir was filled with water to saturate the sand. Following saturation, an overall gradient of 0.02 was established using the constant-head overflow ports in each reservoir chamber. The water level was at a depth of 5 mm at the upstream reservoir and 15 mm at the downstream edge.

After the overall flow gradient was established, the stabilizer was introduced to the formation using delivery wells. The wells were constructed of 19 mm PVC pipe with three 6-mm-diameter injection ports screened with nylon. The ports were arranged in one vertical row at depths of 25, 45, and 65 mm below the sand surface. The ports were placed in the upper half of the wells to permit both gravity and hydraulic flow. Five wells spaced at 50 mm intervals center-to-center were installed by gently pushing them into the sand deposit. The wells were located 150 mm from the upstream edge with the ports facing in the downstream direction. A distribution bay (80 mm × 304 mm in plan by 51 mm high) was placed on top of the wells to maintain a constant supply of colloidal silica to the wells.

The box model experiment was designed based on the results of previous modeling reported in Gallagher and Koch (2003). Previous experiments showed that a low-head injection well adds enough hydraulic gradient to the system to permit both up and down gradient stabilizer flow. Therefore, the location of the injection wells in this model was selected to maximize stabilizer delivery in both the up and down gradient directions. Additionally, since the stabilizer density is slightly greater than the pore water, the wells were screened in the upper third to make use of the density gradient for stabilizer density in the bottom of the model. Furthermore, the previous work showed that when extraction wells were not used, stabilizer traveled through the sand and into the effluent chamber. The addition of extraction wells in this model largely prevented the stabilizer from entering the down gradient water chamber. The extraction wells also served to increase the hydraulic gradient and direct the flow of stabilizer within the sand layer.

During colloidal silica delivery, a constant head of 200 mm as measured from the bottom of the tank was maintained in the delivery wells. This excess head resulted in stabilizer movement in both the upstream and downstream directions. Over a period of 10 h, approximately $1\frac{1}{2}$ pore volumes (about 16 1/2 L) of 5% by weight colloidal silica solution (0.1 N, pH 6.3) were delivered to the formation. The ionic strength of the solution was adjusted using NaCl so that the viscosity of the gel increased by a factor of ten within approximately 10 h after mixing. The colloidal silica

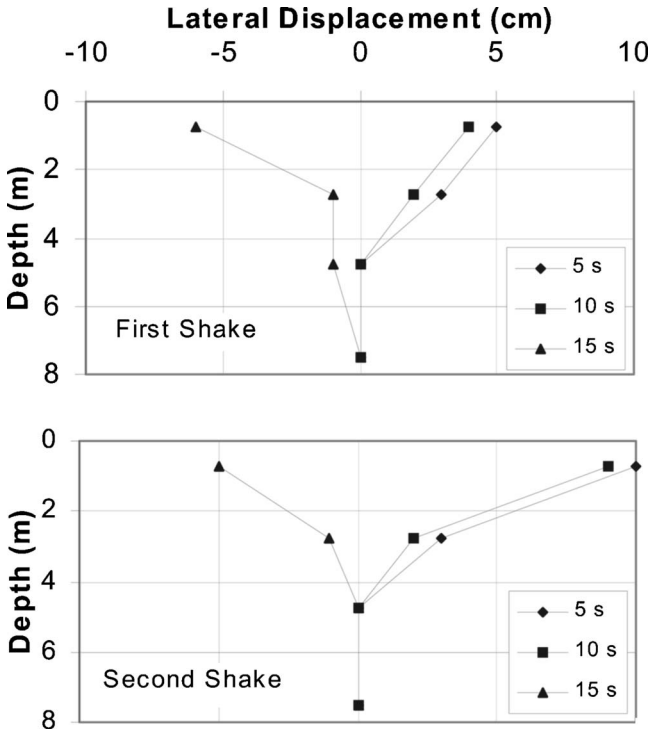

Fig. 10. Measured lateral displacements during shaking events

solution was colored with red food dye so that investigators could visually determine the colloidal silica advancement on the top and sides of the model, as shown in Fig. 12.

Two extraction wells were used to withdraw fluid from the sand formation at a rate of 12 mL/min. The extraction wells were constructed of 19 mm PVC pipe with nine 6-mm-diameter ports screened with nylon. The ports were uniformly distributed along the length of the well, starting at a depth of 25 mm below the sand surface. The wells were installed adjacent to the downstream edge of the model at equally spaced intervals, with the extraction ports facing upstream.

The chloride concentration of the pore fluid was monitored during the course of stabilizer delivery. Pore fluid samples were extracted from the sampling ports at times of 0.75, 2.75, 5, 8.25, and 9.75 h after delivery began. Gallagher and Lin (2005) showed

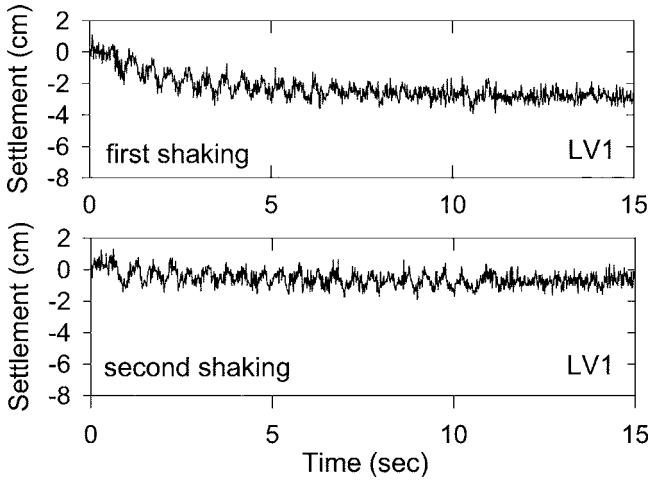

Fig. 11. Measured settlement during shaking events

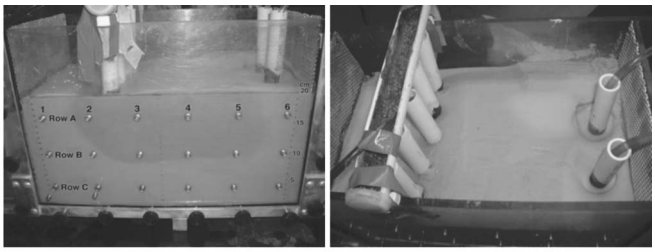

(a) Side view (b) Plan view

Fig. 12. Box model experiment for colloidal silica delivery study. Colloidal silica progression after 3 h. Flow is from left to right.

that chloride is a good indicator of the relative concentration of colloidal silica present in the pore fluid. In general, the chloride concentration increased gradually before the dyed stabilizer solution became visible to the eye. The chloride concentration then increased to the background concentration of the source solution. By the end of colloidal silica delivery, the chloride concentration in the down gradient ports indicated that the silica concentration was very similar to the source solution. After colloidal silica delivery was completed, the model was cured for 14 days and then excavated into six block samples. The six block samples were carved into smaller specimens for unconfined compression testing. Twenty one unconfined compression tests were performed. Unconfined compressive strength ranged from a low of 16 kPa (2.3 psi) to a high of 61 kPa (8.9 psi).

Box Model Results

The chloride concentrations measured in the sampling ports at the end of the experiment indicate of fairly uniform colloidal silica coverage on both sides of the model. Additionally, the unconfined compressive strength results are in general agreement with previous work where the unconfined compressive strength of samples was tested at a known concentration of 5% by weight colloidal silica (Gallagher and Mitchell 2002). The samples from this work showed an average baseline strength of 32 kPa (4.7 psi). The cyclic deformation resistance of sand treated by 5% by weight colloidal silica was shown to be sufficient to effectively mitigate the liquefaction risk. Given the consistent geotechnical behavior of the samples from the box model and those reported by Gallagher and Mitchell (2002), it was concluded that fairly uniform and sufficient coverage was obtained by low-gradient stabilizer delivery.

It is anticipated that in field applications, not all the pores of the formation will be filled with grout. There may be variability in the size of the pores and preferential flow through the formation. It is likely that the larger pores will fill with grout first. Grout will then make its way into smaller pores by dispersion and diffusion. Therefore, the coverage throughout the formation will probably not be uniform. However, if the majority of the pores are filled with grout, the silica bonds between the grains are likely to be enough to hold the particles together and prevent excessive deformation during seismic events.

Discussion

Centrifuge modeling was used to investigate the improvement that can be obtained when liquefiable sand treated with 6% by

weight colloidal silica grout is subjected to in-flight earthquake shaking. Loose sand was successfully saturated with 6% by weight colloidal silica grout and subsequently subjected to two shaking events to evaluate the response of the remediated sand layer. The treated soil did not liquefy during either shaking event. Shear strains of ±0.5 and ±1% were recorded during the first and second shaking events, respectively. The treated soil experienced 30 mm of settlement (0.3% strain) and less than 10 mm (0.1% strain) at the center of the model during the first and second shaking events, respectively. Taboada (1995) measured average prototype settlements of 170–200 mm during shaking, and additional settlements of 30–40 mm during the postshaking period (corresponding to total vertical strains of about 2–2.5%) in similar centrifuge tests (having peak input accelerations of $0.23–0.25g$) done on untreated soil models prepared in the same manner described above. Thus, measured settlements of the treated sand were up to 25 times less than that of the untreated soil models. Postshaking vertical deformations did occur in the untreated sand; however, settlements only increased (Fig. 11) as shaking continued and stopped immediately when shaking stopped in the treated sand. Manual measurements taken after each test showed that vertical deformations were insignificant, indicating that the increase in recorded settlement–time histories (Fig. 11) may have been primarily due to a degrease in height of the soil profile during lateral deformation of the soil mass, rather than settlement due to cyclic-induced densification/settlement that occurred at untreated soil models.

Based on these results and previous work, it is evident that treatment of loose sands with dilute colloidal silica greatly reduces their liquefaction potential. During the centrifuge tests, signal amplification was recorded to depths of 2 and 4 m during the first and second shaking events, respectively. It is thought that this acceleration amplitude could be due to incomplete gelation of the colloidal silica. The colloidal silica gel continues to gain strength with time as additional silica bonds form between each other and the sand particles. Pamuk (2004) indicated that the longer the delay between treatment and shaking, the less ground motion amplification could be expected. A second explanation for the amplification is the potential degradation in the particles adhesion provided by the cementation from the colloidal grout. Previous triaxial tests indicated that this degradation could be improved by increasing the concentration of the grout. However, this phenomenon is likely to be encountered with most forms of chemical stabilization. Even with some degradation of chemical bonds, it is expected that the soil formation would provide adequate liquefaction resistance. If local deformation were to occur, it would likely be centered in areas that had lower concentrations of colloidal silica treatment. Overall deformation of the treated layer would still be expected to be minimal compared to an untreated layer.

The primary feasibility issue remaining for field implementation of passive site stabilization is uniform delivery of the stabilizer to the target location. The results of this and other box model tests (Gallagher and Koch 2003) were generally successful in demonstrating that colloidal silica can be delivered to a uniform loose sand formation using low-head injection and extraction wells. Stabilizer delivery is driven by both the density of the stabilizer and the hydraulic gradient. The density difference between the stabilizer and the groundwater causes gravity flow, which assists in delivering the stabilizer to the bottom of the treatment zone. Extraction wells at the down gradient edge increased the hydraulic gradient and increase the speed of stabilizer delivery.

Conclusions

A physical modeling tool was used to measure the liquefaction resistance and deformation behavior of the colloidal silica-treated sand deposit. The results of this research will be used to continue the investigation of uniform stabilizer delivery. One issue to be studied includes in-flight delivery of grout. By injecting grout in-flight, the physical processes can be modeled more accurately, particularly the effects of confining pressure on low-gradient stabilizer delivery. A second area to be investigated is the treatment that can be achieved by injecting 1 pore volume of grout. As noted earlier, cost-effective treatment requires that the minimum amount of material be used. Therefore, the amount of coverage that can be achieved with 1 pore volume of stabilizer must be determined.

Colloidal silica has great potential as an innovative material for cost-effective stabilization of liquefiable soils. It is nontoxic and is expected to be chemically stable under typical subsurface conditions. In low concentrations, it greatly increases the deformation resistance of loose sands subjected to earthquake shaking. Passive site stabilization is a new method of ground improvement that could have broad application for developed sites susceptible to liquefaction. It could be used in place of traditional grouting methods to treat entire sites rather than targeted structures. In this way, both structures and their associated lifelines could be protected from disruption due to earthquake shaking.

Acknowledgments

The writers would like to thank Yuanzhi Lin, Waleska Mora, and Kathy Quinn for running the box model experiments and Stefan Finsterle and Jennifer Schaeffer for their thoughtful reviews of the manuscript. This research was funded by the National Science Foundation through the Multi-Disciplinary Center for Earthquake Engineering Research (MCEER) Research Project No. 01-2033, Task 2.3, Geotechnical Rehabilitation: Site and Foundation Remediation.

References

Arulanandan, K., and Scott, R., eds. (1993). *Verification of numerical procedures for the analysis of soil liquefaction problems*, Balkema, Rotterdam, The Netherlands.

Bartlett, S. F., and Youd, T. L. (1992). "Case histories of lateral spreads caused by the 1964 Alaska earthquake." *Case studies of liquefaction and lifeline performance during past earthquake: United States case studies*, T. D. O'Rourke and M. Hamada, eds., Chap. 2, *Technical Rep. No. NCEER-92–0002*, National Center for Earthquake Engineering Research, Univ. of Buffalo, Buffalo, N.Y., 2-1–2-127.

Dobry, R., and Abdoun, T. (1998). "Post-triggering response of liquefied sand in the free field and near foundations." *Proc., Geotechnical Earthquake Engineering and Soil Dynamics III Conf.*, ASCE, Reston, Va., 270–300.

Dobry, R., and Abdoun, T. (2001). "Recent studies on seismic centrifuge modeling of liquefaction and its effects on deep foundations." *Proc., 4th Int. Conf. on Recent Advances in Geotechnical Earthquake Engineering and Soil Dynamics*, San Diego.

Gallagher, P. M., and Koch, A. J. (2003). "Model testing of passive site stabilization: A new grouting technique." *Grouting and Ground Treatment: Proc., 3rd Int. Conf.*, ASCE, Reston, Va., 1478–1489.

Gallagher, P. M., and Lin, Y. (2005). "Column testing to determine colloidal silica transport mechanisms." *Innovations in grouting and soil*

improvement, ASCE, Reston, Va., 15–26.
Gallagher, P. M., and Mitchell, J. K. (2002). "Influence of colloidal silica grout on liquefaction potential and cyclic undrained behavior of loose sand." *Soil Dyn. Earthquake Eng.*, 22(9–12), 1017–1026.
Gallagher, P. M., Pamuk, A., Koch, A. J., and Abdoun, T. H. (2002). "Centrifuge Modeling of Passive Site Remediation." *Proc., 7th United States National Conf. on Earthquake Engineering (7NCEE): Urban Earthquake Risk*, Earthquake Engineering Research Institute, Oakland, Calif.
Hamada, M., and O'Rourke, T. D. (1992). "Case histories of liquefaction and lifeline performance during past earthquakes." *Technical Rep. No. NCEER-92-0001*, National Center for Earthquake Engineering Research, Univ. of Buffalo, Buffalo, N.Y.
Hamada, M., Wakamatsu, K., and Ando, T. (1996). "Liquefaction-induced ground deformation and its caused damage during the 1995 Hyogoken-Nanbu earthquake." *Proc., 6th Japan-United States Workshop on Earthquake Resistant Design of Lifeline Facilities and Countermeasures against Soil Liquefaction*, *Technical Rep. No. NCEER-96–0012*, National Center for Earthquake Engineering Research, Univ. of Buffalo, Buffalo, N.Y., 137–152.
Hamada, M., Yasuda, S., Isoyama, R., and Imoto, K. (1986). *Study on liquefaction-induced permanent ground displacements*, Association for the Development of Earthquake Prediction, Tokyo.
Iler, R. K. (1979). *The chemistry of silica: Solubility, polymerization, colloid, and surface properties, and biochemistry*, Wiley, New York.
Ishihara, K., Yasuda, S., and Nagase, H. (1996). "Soil characteristics and ground damage." *Soils Found.*, Special, January, 109–118.
Liao, H. J., Huang, C. C., and Chao, B. S. (2003). "Liquefaction resistance of a colloid silica grouted sand." *Grouting and ground treatment: Proc. 3rd Int. Conf.*, ASCE, Reston, Va., 1305–1313.
National Research Council (NRC) (1985). "Liquefaction of soils during earthquakes." *Rep. No. CETS-EE-001*, Committee on Earthquake Engineering, National Academy Press, Washington, D.C.
O'Rourke, T. D., and Hamada, M. (1992). "Case studies of liquefaction and lifeline performance during past earthquakes: United States case studies." *Tech. Rep. No. NCEER-92–0002*, National Center for Earthquake Engineering Research, Univ. of Buffalo, Buffalo, N.Y.
Pamuk, A. (2004). "Physical modeling of retrofitted pile groups including passive site remediation against lateral spreading." Ph.D. thesis, Rensselaer Polytechnic Institute, Troy, N.Y.
Persoff, P., Apps, J., Moridis, G., and Whang, J. M. (1999). "Effect of dilution and contaminants on sand grouted with colloidal silica." *J. Geotech. Geoenviron. Eng.*, 125(6), 461–469.
Taboada, V. M. (1995). "Centrifuge modeling of earthquake-induced lateral spreading in sand using a laminar box." Ph.D. thesis, Rensselaer Polytechnic Institute, Troy, N.Y.
Whang, J. M. (1995). "Section 9—Chemical-based barrier materials." *Assessment of barrier containment technologies for environmental remediation applications*, R. R. Rumer and J. K. Mitchell, eds., NTIS, Springfield, Va., 211–247.
Yonekura, R., and Kaga, M. (1992). "Current chemical grout engineering in Japan." *Proc., Grouting, Soil Improvement and Geosynthetics*, ASCE, New York, 725–736.